Current oscillations, switching, and hysteresis in CdSe nanorod superlattices

Hugo E. Romero, Gregory Calusine, and Marija Drndic*
Department of Physics and Astronomy, University of Pennsylvania, Philadelphia, Pennsylvania 19104, USA
(Received 20 April 2005; revised manuscript received 15 July 2005; published 1 December 2005)

CdSe quantum rod (QR) arrays show striking and anomalous transport properties below 300 K. Strong and reproducible nonlinearities, including current oscillations with dc voltage, are observed in the current-voltage characteristics above a temperature-dependent threshold. The observations are tentatively interpreted as due to resonant tunneling of charge carriers between adjacent QR wells via localized states in insulating barriers.

DOI: 10.1103/PhysRevB.72.235401 PACS number(s): 05.60.Gg, 73.21.−b, 73.63.Kv

I. INTRODUCTION

Colloidal semiconductor nanocrystals (NCs), also known as "quantum dots" (QDs), are of great interest for both fundamental research and technical applications in optoelectronic devices and nanotechnology, due to their strong size-dependent electrical and optical properties.[1] Shape control of such NCs was achieved by the manipulation of the growth kinetics to produce rodlike structures—nanorods or quantum rods (QRs).[2]

Semiconductor QRs are expected to exhibit interesting behavior because of their well-defined shape with the long axis preferably grown along the unique c axis. For instance, it has been demonstrated that CdSe QRs emit linearly polarized light along the c axis.[2] QRs would also allow for efficient quasi-1D electrical transport. Thus, when organized into arrays of aligned QRs, improved and unconventional electronic transport could be achieved compared to that of "spherical" NC arrays. In addition, by tuning the aspect ratio of QRs, one can study the transition from zero- to one-dimensional quantum-confined systems.

We report on interesting electrical transport phenomena in CdSe QR arrays. Anomalous nonlinearities in the current-voltage I-V_{bias} curves consist of two main features: (i) discontinuous switching events accompanied by hysteresis, and (ii) periodic current oscillations as a function of V_{bias}. The evidence indicates that CdSe QR arrays may behave as semiconductor-insulator multiple wells.

II. EXPERIMENTAL DETAILS

CdSe QRs, passivated with a 1.1-nm layer of tri-n-octyl-phosphine oxide (TOPO), were synthesized according to the previously published CdO one-pot procedure.[3,4] They were purified and size-selected by centrifugation. Transmission electron microscopy (TEM) images (Fig. 1) revealed that the final product contained nearly monodispersed CdSe QRs with an average length of 18 ± 1 nm and average diameter of 5.2 ± 0.3 nm (i.e., aspect ratio of ~3.5). The clear lattice fringes observed in high-resolution TEM images are indicative of good crystallinity.

CdSe QR *monolayers* were prepared by drop casting a 3:1 toluene-butyl ether solution onto lithographically pre-patterned Si substrates covered with a 300-nm layer of SiO_2. The doped Si substrate was used as an electrically grounded back gate. The patterns are arrays of paired 800-μm-wide Ti/Au electrodes with a gap of $l=1-2$ μm. Prior to film deposition, the Si substrates were treated for 10 min under O_2 plasma to reduce organic surface contamination. The isolation between the contact pads before film deposition was >10 PΩ at 300 K, and even higher at lower T.

Electrical transport measurements were carried out as a function of T, while *warming up* from 77 to 300 K, in a LN_2 cryostat under a dynamic vacuum of $<10^{-6}$ Torr. T was controlled with ±0.5 K accuracy. A bias voltage V_{bias} was applied to the source electrode at ramp rates of $\sim5-25$ mV/s, and the current I at the drain was monitored with a virtual-earth current amplifier. The current detection limit in our measurements is ~5 fA. We present the results from two typical samples, identified as device A ($l=1$ μm) and device B ($l=2$ μm). The behavior reported here was observed in *all* eight samples that we studied.

III. RESULTS AND DISCUSSION

Figure 2 shows I-V_{bias} characteristics as a function of T for device A. The current increases smoothly with V_{bias}. At $T>200$ K, as V_{bias} is increased above a sharply defined threshold voltage V_T, the current jumps discontinuously to a higher value, i.e., there is a transition to a *high-conducting* state.[5] As V_{bias} is reduced below another characteristic value V_T^*, the sample switches back to the original *low-conducting* state, resulting in a well-resolved hysteretic effect, as shown in the inset to Fig. 2 for $T=250$ K. All hysteretic loops observed in the I-V_{bias} curves are counterclockwise, i.e., $V_T \geqslant V_T^*$.

Beyond V_T and for $T<250$ K, linear conduction is observed and the high-V_{bias} current often extrapolates back to zero at $V_{bias}=0$. However, for $T>260$ K, the I-V_{bias} curves become increasingly nonlinear, both below and above V_T.

Figure 3 displays I-V_{bias} characteristics as a function of T for device B, at both positive and negative V_{bias}. These curves illustrate the asymmetry of the I-V_{bias} characteristics with respect to V_{bias} polarity, which is fairly common in our samples. Moreover, V_T values are larger for negative V_{bias} at a fixed T. This could result from an asymmetry in the potential profile in the presence of a grounded back gate, although its origin is not clear at this moment.

Also apparent in Fig. 3 is that the region around the current jump from the low- to high-conducting state is unstable,

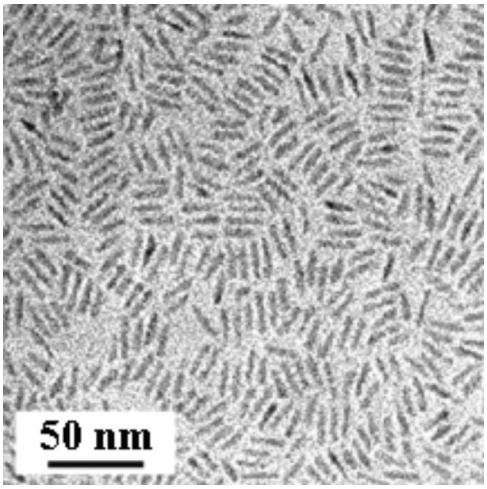

FIG. 1. TEM images of a CdSe QR sample, showing a narrow size distribution of ~5%. Counting over 300 QRs resulted in an average length of 18±1 nm and an average diameter of 5.2±0.3 nm.

resulting in frequent multiple switching events between the two states in a single I-V_{bias} curve. No switching events have been observed, at any T, outside the threshold region.

Comparison of I-V_{bias} curves for device A (Fig. 2) and device B (Fig. 3) indicates that V_T is dependent on sample size l, i.e., V_T increases with l at a fixed T. V_T is also T dependent, as seen in Fig. 4, and follows the empirical relation $V_T \sim \exp(-T/T_0)$ with a characteristic T_0=18 and 20 K for device A (l=1 μm) and B (l=2 μm), respectively. Interestingly, this empirical $V_T(T)$ dependence is frequently observed for depinning of charge-density waves in $NbSe_3$.[6]

The most remarkable feature of the I-V_{bias} curves in Figs. 2 and 3 is the appearance of periodic current oscillations as a function of V_{bias}, superimposed on a dc current. The current

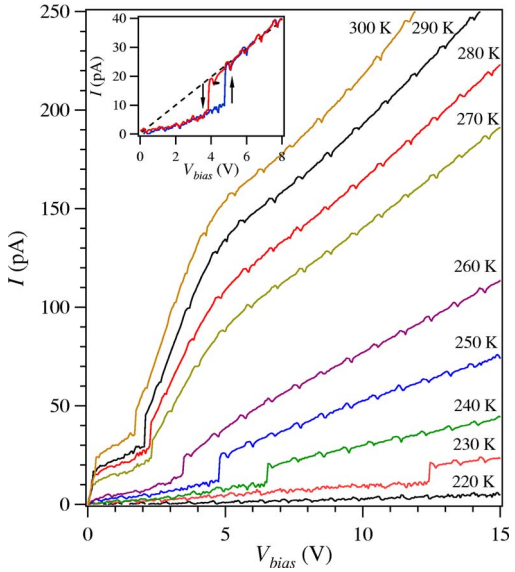

FIG. 2. (Color online) Typical I-V_{bias} characteristics as a function of T for device A (l=1 μm). Only forward bias traces are shown for clarity. The inset displays a typical hysteretic loop. The arrows show the direction of the V_{bias} sweep.

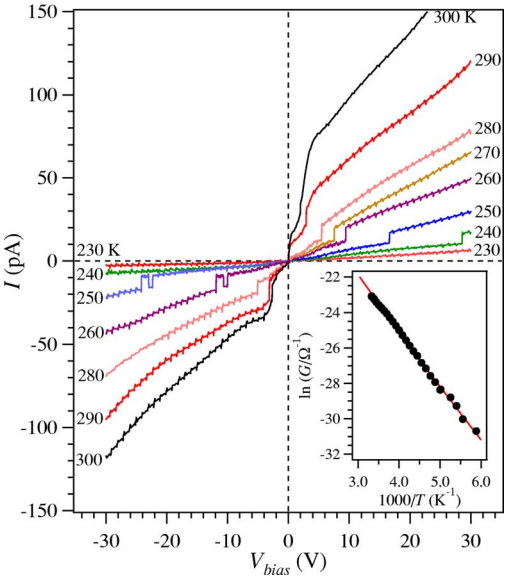

FIG. 3. (Color online) Typical I-V_{bias} characteristics as a function of T for device B (l=2 μm). Only forward bias traces are shown for clarity. Notice the multiple switching events at $V_{bias} \sim V_T$ for curves taken at 250 and 260 K. The inset shows the temperature dependence of the zero-bias conductance G.

oscillations are observed for V_{bias} as high as 50 V, and persist in the high-conducting region as the V_{bias} is decreased again toward zero.

What is clearly visible in the I-V_{bias} characteristics in Figs. 2 and 3 is that the current oscillations are strongly pronounced for $V_{bias} > V_T$. Below V_T, current fluctuations typically appear in the form of random and aperiodic noise.

Three periods of the current oscillations are shown in the upper inset to Fig. 5. The main features are the sawtoothlike oscillation and the small steps before and after each oscillation. The amplitude of the oscillations $\Delta I \sim 2$ pA is nearly constant at all T. However, the voltage periodicity ΔV_{bias} of the current oscillations, as defined in the upper inset to Fig. 5, usually seems to increase linearly with T (Fig. 5, lower inset), but the T range is too narrow to determine with certainty the functional dependence of $\Delta V_{bias}(T)$. In contrast to V_T, $\Delta V_{bias} \sim 1$ V is independent on sample size l.

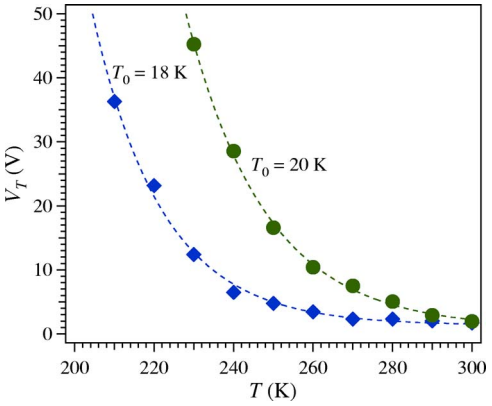

FIG. 4. (Color online) Temperature dependence of the threshold voltage V_T for devices A (diamonds) and B (circles).

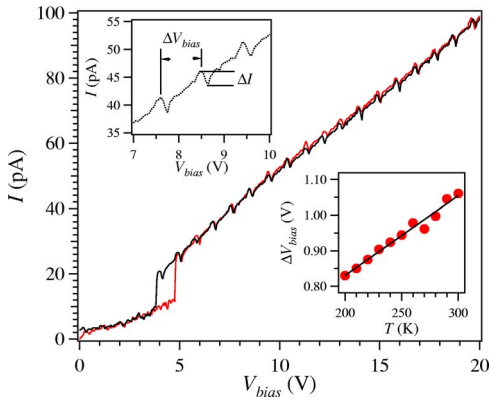

FIG. 5. (Color online) I-V_{bias} characteristics at 250 K for device A. The upper inset is an expanded view of the I-V_{bias} in a limited V_{bias} range, showing the regular periodicity of the current oscillations. The lower inset shows the periodicity ΔV_{bias} of current oscillations as a function of T. ΔV_{bias} was determined from an average of over 50 periods.

Because the switching and hysteresis in our arrays primarily occurs for $I<50$ pA at V_{bias} as low as 100 mV (i.e., power levels are restricted to pW), it is rather unlikely that electron heating is responsible for the effects seen in Figs. 2 and 3. Moreover, the overall shape of the I-V_{bias} is independent of the V_{bias} sweeping rate. On the other hand, since the I-V_{bias} curves are highly reproducible during consecutive measurements within a cooldown and rather "stable" during very slow sweeps, these effects may not be related to changes in occupation of impurity states. In addition, we did not observe a time-dependent increase of I under constant-V_{bias} conditions above V_T, characteristic of the impact ionization phenomena.

The nonlinear and the oscillatory behavior of the I-V_{bias} characteristics reported here are qualitatively similar to what has been seen in studies on miniband transport and sequential resonant tunneling in two-dimensional (2D) semiconductor superlattices exhibiting negative differential resistance (NDR).[7,8] If the electron density in such systems is large, the uniform electric-field distribution becomes unstable at the onset of the NDR region and two domains of different electric-field strength are formed. The formation of electric-field domains usually results in a series of periodic oscillations or infinitesimally sharp discontinuities as a function of V_{bias} above a threshold in the I-V_{bias} curves, with a voltage period which is sample size independent and roughly reflects the spacing of the electronic subbands of the superlattice. Similar effects are also expected in superlattices of lower dimensionality.[9]

Usually, long tracks of CdSe QRs stacked side-by-side are spontaneously formed upon deposition of CdSe QRs on a substrate from a solution by slow solvent evaporation (Fig. 6). The attractive dipolar interactions between adjacent QRs might be the driving force for formation of QR tracks.[10,11] At high concentrations, these tracks may align parallel to each other, resulting in smectic-A ordered superstructures.[12] In some cases, CdSe QRs can connect to each other head-to-tail to form linear arrays.[11]

We believe that the self-assembly of QRs into these superlattice structures plays an important role in the electronic

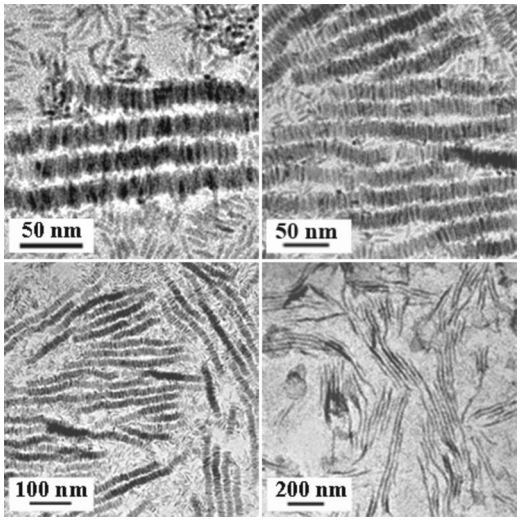

FIG. 6. TEM images of typical CdSe QR superlattices formed when CdSe QRs are deposited by slow solvent evaporation method on thin films of amorphous carbon supported by a copper grid. CdSe QRs have strong preference for self-assembly into separate closed-packed "stacks," in which QRs align with their long axis parallel to each other. The long tracks of QR stacks may align parallel to each other, resulting in smectic ordered superstructures.

conduction in QR arrays and a model to explain the nonlinearities observed in the I-V_{bias} characteristics must take into account this ordering. In fact, the behaviors reported here (i.e., current oscillations and switching) are not readily observed in more disordered CdSe QR arrays; typically prepared by fast solvent evaporation method.

Even though enhanced conduction should be expected along the long axis of the QRs, dipole-dipole interactions may lead to better and stronger electronic coupling between QRs aligned side by side than those connected head to tail. Thus it is likely that the current is, in general, confined to a few major percolating paths through laterally coupled QRs where side-by-side tunneling is the dominant transport mechanism.

At this point, it is instructive to understand the origin of charge carriers in the system. The zero-bias conductance G (Fig. 3, inset) increases with increasing T.[13] Above 220 K, the T dependence is consistent with thermionic emission of electrons into the conduction band of CdSe QRs, across the barriers at the electrodes. $G(T)$ is then well described by the relation $G(T)\approx G_0 T\exp(-\varphi/k_B T)$ over three decades in G, with a barrier height $\varphi\sim 0.25$ eV. This is consistent with the estimated energy difference between the work function of Au and the ground level of the conduction band in the QRs.

The formation of periodic current oscillations as a function of V_{bias} can be tentatively interpreted by assuming that CdSe QR form superlattices consisting of a periodic arrangement of N quantum wells (i.e., the QRs) separated by insulating barriers formed by the TOPO ligands. For nonzero V_{bias} across the sample, charges injected at the electrodes can tunnel from well to well and transfer the energy gained due to the electric field (e.g., to the lattice vibrations in phonon-assisted tunneling). This leads to a space-charge buildup near the source. The space-charge buildup screens the external

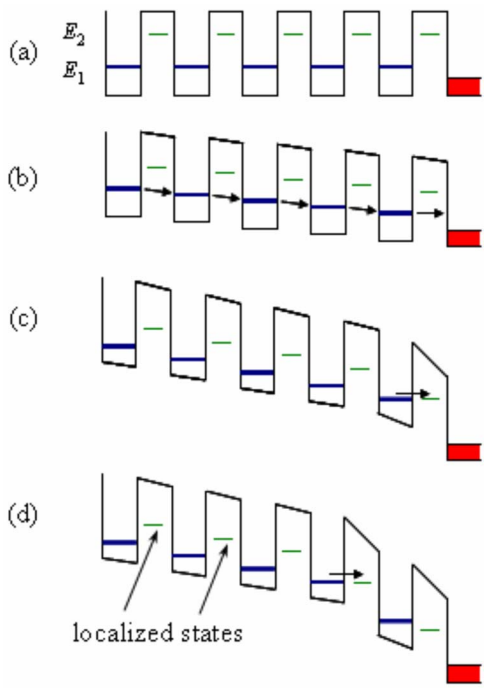

FIG. 7. (Color online) Schematic conduction band profile of a semiconductor (CdSe QR)-insulator (TOPO) superlattice for several values of the average potential per period ΔV_{bias}. (a) Zero bias. (b) Direct tunneling through ground state E_1; arrows indicate electron transport. (c) First resonant tunneling occurs through localized state in the insulating barrier. (d) Second resonant tunneling.

electric field creating a nonuniform electric field across the sample; the voltage drop is larger across QR wells further away from the source than for those close to it. A measurable current results from electrons tunneling from the space-charge region near the source electrode into the unoccupied states towards the drain electrode.

At high enough fields, in addition to direct tunneling through the insulating barriers, resonant tunneling between neighboring QRs via localized electronic states in the insulating TOPO ligands could be possible.[14]

This can be understood with the aid of the conduction-band diagram of a semiconductor-insulator superlattice (Fig. 7). When the ground state in the nth QR well at E_1 is aligned with the available state in the barrier at E_2, a resonant condition can occur where electrons from the nth QR well tunnel to the barrier followed by a rapid relaxation to the ground state at the $(n+1)$th QR well. This gives rise to a peak in the current at energies $e\Delta V_{bias}=E_1-E_2$. This peak is followed by a current decrease as V_{bias} is increased further and the resonant condition is no longer satisfied. The oscillation repeats itself as the localized state in the next barrier aligns with the ground level of the $(n-1)$th QR well.[15]

As mentioned above, the voltage difference between the current oscillations is sample size independent and given by $e\Delta V_{bias}=E_1-E_2\sim 1$ eV, consistent with the barrier height created by TOPO ligands, as estimated from photocurrent measurements.[16]

The origin of localized states in TOPO is uncertain. The most compelling candidates are the highest occupied molecular orbital (HOMO) and the lowest unoccupied molecular orbital (LUMO), yet these important parameters are difficult to determine. Several reports have provided strong evidence for resonant tunneling via discrete and localized molecular orbitals in organic molecules.[17–20]

Localized molecular states could be also formed by chemical reactions between the TOPO molecules and Cd atoms in the QR surface. Unfortunately, the bonding in adducts of phosphine oxides with metal atoms is a complex subject and, in general, the extent to which the molecular nature of the surface affect the electronic properties of NCs and QRs is not well understood. Nevertheless, it is clear that the surface may in some instances play a significant role.[21]

IV. SUMMARY

In summary, we have demonstrated the emergence of hysteretic and switching behavior and striking periodic current oscillations as a function of voltage bias in the I-V_{bias} characteristics of CdSe nanorod superlattices consisting of long tracks of parallel nanorods. The period of the oscillations is sample size independent, but weakly temperature dependent. A possible scenario that can lead to the periodic oscillatory behavior assumes that the CdSe nanorod superlattices behave as semiconductor-insulator multiple quantum wells with localized states in thin insulating barriers, where resonant tunneling of electrons via these localized states is the dominant transport mechanism.

This work opens a range of outstanding questions that can be addressed in this system. The period of current oscillations should depend on the details of the insulating barriers and this will be explored by changing the ligands using well-established chemical procedures. More detailed studies of the observed hysteresis and switching are also underway and will be presented in subsequent publications. Other questions include the importance of structural order in nanorod superlattices. This order could be controlled by a choice of solvents. Nanorod assembly patterns, including ordered phases and topological defects, and their arrangement relative to the electrodes might leave imprints on the I-V_{bias} characteristics. Microscopic mechanism should be further explored by measuring smaller nanorod superlattices (from single nanorods to linear nanorod chains and small square arrays) with well-controlled properties.

Undoubtedly, the controllable nature of semiconductor nanorod superlattices provides a useful system in which to experimentally explore general models of coupled quantum well systems, correlated electrons, and charge ordering. In addition, considering a possible interplay between electrical and optical effects, these results might stimulate further interesting electronic-optoelectronic applications of CdSe nanorods.

ACKNOWLEDGMENTS

This work was funded in part by the ONR (Grant No. N000140410489), the ACS (Grant No. 41256-G10), and NSF Grant Nos. NSEC DMR-0425780 and DMR-0449553.

*Author to whom correspondence should be addressed. Email address: drndic@physics.upenn.edu

[1] A. P. Alivisatos, Science **271**, 933 (1996).
[2] X. Peng, U. Manna, W. Yang, J. Wickham, E. Scher, A. Kadavanich, and A. P. Alivisatos, Nature (London) **404**, 59 (2000).
[3] Z. A. Peng and X. Peng, J. Am. Chem. Soc. **123**, 183 (2001).
[4] Z. A. Peng and X. Peng, J. Am. Chem. Soc. **124**, 3343 (2002).
[5] Below 200 K, the sample shows only a nonconducting state where $I \sim 0$ in the entire V_{bias} range (±50 V).
[6] $T_0 \sim 17$ K has been measured in $NbSe_2$ nanowires (see, for example, Refs. 22 and 23).
[7] L. Esaki and L. L. Chang, Phys. Rev. Lett. **33**, 495 (1974).
[8] K. K. Choi, B. F. Levine, R. J. Malik, J. Walker, and C. G. Bethea, Phys. Rev. B **35**, 4172 (1987).
[9] M. Zwolak, D. Ferguson, and M. DiVentra, Phys. Rev. B **67**, 081303(R) (2003).
[10] S. D. Bunge, K. M. Krueger, T. J. Boyle, M. A. Rodriguez, T. J. Headleya, and V. L. Colvin, J. Mater. Chem. **13**, 1705 (2003).
[11] L.-S. Li and P. Alivisatos, Adv. Mater. (Weinheim, Ger.) **15**, 408 (2003).
[12] D. V. Talapin, E. V. Shevchenko, C. B. Murray, A. Kornowski, S. Forster, and H. Weller, J. Am. Chem. Soc. **126**, 12984 (2004).
[13] G measurements were carried out by sweeping V_{bias} up and down in the range ±50 mV, after reaching thermal equilibrium at a fixed T and calculating the derivative of the resulting I-V_{bias} curves at $V_{bias}=0$.
[14] Current oscillations as a function of V_{bias}, resulting from resonant tunneling in dc I-V_{bias} curves at relatively high electric fields, were theoretically predicted in semiconductor-insulator multiple quantum wells assuming localized states in thin insulator barriers, such as in Si/SiO_2 superlattices.[24]
[15] N current peaks should be expected for a 1D superlattice with N wells. We observe current oscillations up to the maximum applied $V_{bias} \sim 50$ V.
[16] C. A. Leatherdale, C. R. Kagan, N. Y. Morgan, S. A. Empedocles, M. A. Kastner, and M. G. Bawendi, Phys. Rev. B **62**, 2669 (2000).
[17] F.-R. F. Fan, R. Y. Lai, J. Cornil, Y. Karzazi, J.-L. Bredas, L. Cai, L. Cheng, Y. Yao, D. W. Price, S. M. Dirk, J. M. Tour, and A. J. Bard, J. Am. Chem. Soc. **126**, 2568 (2004).
[18] R. A. Wassel, G. M. Credo, R. R. Fuierer, D. L. Feldheim, and C. B. Gorman, J. Am. Chem. Soc. **126**, 295 (2004).
[19] N. J. Tao, Phys. Rev. Lett. **76**, 4066 (1996).
[20] L. Scudiero, D. E. Barlow, U. Mazur, and K. W. Hipps, J. Am. Chem. Soc. **123**, 4073 (2001).
[21] S. Pokranta and K. B. Whaleyb, Eur. Phys. J. D **6**, 255 (1999).
[22] O. C. Mantel, F. Chalin, C. Dekker, H. S. J. V. der Zant, Y. Latyshev, B. Pannetier, and P. Monceau, Synth. Met. **103**, 2612 (1999).
[23] Y. S. Hor, Z. L. Xiao, U. Welp, Y. Ito, J. F. Mitchell, R. E. Cook, W. K. Kwok, and G. W. Crabtree, Nano Lett. **5**, 397 (2005).
[24] A. N. Kholod, V. E. Borisenko, A. Zaslavsky, and F. A. d'Avitaya, Phys. Rev. B **60**, 15975 (1999).